

DT-MRI measurement of myolaminar structure: accuracy and sensitivity to time post-fixation, b-value and number of directions*

Stephen H. Gilbert, Bruce H. Smaill, Richard D. Walton, Mark L. Trew† and Olivier Bernus‡.

Abstract— DT-MRI has been widely used to quantify myocardial fiber and laminar orientations. These structural orientations influence both the spread of excitation and the reorganization of the myocardium during contraction and are altered in disease states. Studies have sought to validate DT-MRI but questions remain about the accuracy of the method and its sensitivity to the time post-fixation and imaging parameters, including *b*-value, number of diffusion directions and image voxel size. The advent of high-spatial resolution *ex vivo* MRI and structure tensor (ST) analysis provides a means of direct validation of DT-MRI and assessment of sensitivity to the *b*-value, the number of diffusion directions and the image voxel size. We find that, with the fixation method we used, structure does not change with time (up to 72 hours). We show that DT-MRI and ST/HR-MRI are markedly similar measures of fiber orientation but DT-MRI and ST are much less similar measures of laminar orientation. DT-MRI performance is not sensitive to the number of directions, with similar structural orientations measured with 6 or 12 directions. Likewise, DT-MRI performance is generally insensitive to *b*-value, but laminar measurement is moderately more accurate at $b = 500$ than for higher *b*-values.

I. INTRODUCTION

The cardiac ventricles have a specialized architecture consisting of a regular fiber-orientation which courses through a conserved and complex myolaminar arrangement (these structures are also known as laminae or sheets). Measurement of orientations of both the fibers and laminae is of interest because they have roles in electrophysiological and biomechanical function in health and disease. Changes in fiber orientation and myolaminar sliding are thought to be the principle mechanisms of myocardial thickening in systole [1-3]. Fiber orientation influences the spread of myocardial activation and laminar organization also substantially influences activation [4]. In the rat, myofiber and myolaminar structure are present

throughout the myocardium (except in the immediate sub-epicardium)[5] and three principal orthogonal structural directions are present: (i) along the fiber axis; (ii) perpendicular to the fiber axis in the sheet plane; and (iii) normal to the sheet plane - a structural arrangement is known as orthotropy [4]. Whole-heart computational modeling requires detailed structural atlases and DT-MRI is often the method of choice for generating these geometries [6]. It has been proposed that DT-MRI can be used to measure both cardiac fiber and laminar orientations [7, 8], however, questions remain about the accuracy of DT-MRI derived laminar orientation, and, to a lesser degree, fiber orientation. Studies have been carried out to validate DT-MRI fiber and laminar orientation measurement [9, 10], with more recent work using structure tensor (ST) analysis of high-resolution MRI (HR-MRI) images [11]. Despite these studies the microanatomical feature imaged in DT-MRI and the sensitivity of these measurements to DT-MRI imaging parameters (such as number of gradient directions and the *b*-value) has not been precisely determined. A monoexponential diffusion model is used in all conventional DT-MRI studies, assuming there is a single diffusion compartment in each voxel. However, importantly, it has been demonstrated in *ex vivo* perfused hearts that there are multiple diffusion components in the myocardium (i.e. nonmonoexponential diffusion, with more than one spin compartment) [12, 13]. These have been classified as a slow component and a fast component [12]. The slow component has been attributed to compartmentalization of intra- and extracellular water pools and the fast component to diffusion in the vascular space compartment combined with some intracellular diffusion [12]. At low *b*-values ($< 1000\text{s/mm}^2$) the fast-component of diffusion predominates, and still influences orientation measurements at higher *b*-values. As it is known that blood vessels generally run parallel to myocardial fibers [14], the effect of summation of the direction of slow and fast diffusion in the standard monoexponential diffusion model is not an important practical concern for the measurement of fiber orientation; and indeed it has been shown that the fiber orientations calculated from the fast and slow components of diffusion are related [12]. However, a consequence of two-component diffusion is that the orthotropic diffusion that has been proposed may be complicated by non-orthotropic fast diffusion which could result in inaccurate measures of laminar orientation. The aim of this study is to examine the sensitivity of the monoexponential diffusion model to imaging parameters by assessing accuracy against high-spatial resolution MRI (HR-MRI) images of the same heart. It has recently been

* This work was supported in part by grants from the Medical Research Council (G0701785, S. H. Gilbert) and the EU FP7 Marie Curie Program PIEF-GA-2010-275261. S.H. Gilbert is the corresponding author † O. Bernus and M.L. Trew contributed equally to this study.

S.H. Gilbert, R. D. Walton and O. Bernus are with the Inserm U1045 - Centre de Recherche Cardio-Thoracique, L'Institut de rythmologie et modélisation cardiaque, Université Bordeaux Segalen, Centre Hospitalier Universitaire de Bordeaux, PTIB - campus Xavier Arnoz, Avenue du Haut Leveque, 33604 Pessac, France, steve.gilbert@ihu-liryc.fr, richard.walton@u-bordeaux2.fr, olivier.bernus@u-bordeaux2.fr.

B.H.Smaill and M.L. Trew are with the Auckland Bioengineering Institute, The University of Auckland, UniServices House, Level 6, 70 Symonds Street, City Campus, Auckland 1010, New Zealand, Auckland, New Zealand. B.H. Smaill is also with the Department of Physiology, University of Auckland, Auckland, New Zealand.

shown that DT-MRI determined fiber orientation changes with time post embedding in *ex vivo* fixed non-perfused hearts, although the global architectural organization does not change [15]. We have therefore explored the sensitivity of orientation measurements to time post-fixation for both DT-MRI and HR-MRI.

II. METHODS

A. Heart Preparation and Perfusion Fixation

Full details are provided in [11], briefly, a male Wistar rat weighing 336 g was euthanized in accordance with the UK Home Office Animals (Scientific Procedures) Act 1986, the heart removed and retrograde perfused with: (i) HEPES-Tyrodes to clear blood; (ii) 2,3-Butanedione 2-monoxime (BDM) to prevent contraction; then (iii) MRI contrast agent (0.1% Gd-DTPA) and fixative (4% formaldehyde). The heart was imaged 2 hours after fixation.

B. HR-MRI and DT-MRI Acquisition and Reconstruction

A series of imaging experiments were carried out (at 20°C) in order to explore sensitivity of measurement to time, *b*-value, and number of gradient directions (Table I). DT-MRI was carried out using the same spectroscope with a set of 6 or 12 optimized directions using a 3D diffusion-weighted spin-echo sequence with TE = 15 ms, TR = 500 ms, at a resolution of 200 x 200 x 200 μm . HR-MRI was carried out using a FLASH (Fast Low Angle SHot) MRI sequence in a Bruker (Ettlingen, Germany) 9.4T spectroscope with 20 averages and echo time (TE) = 7.9 ms repetition time (TR) = 50 ms, with 20 averages taking 18h to acquire at a resolution of 50 x 50 x 50 μm .

C. Comparison of Structure Tensor and Diffusion Tensor Orientations

The structure tensor analysis was described in [16]. No registration was required as the heart was not moved during the 72 hours of imaging, and the MRI voxel dimensions allowed simple alignment. A model cardiac geometry, with a manually fitted LV long-axis, was registered to the heart MRI by affine registration (as in [16]). The orientation angles reported are defined in detail in [17]. Elevation angles are measured from the cardiac short-axis (SA) plane. The fiber helix angle (α_H) is the angle between the transverse plane and the projection of the fiber vector onto the circumferential-longitudinal plane. The fiber transverse angle (α_T) is the angle between the circumferential-longitudinal plane and the projection of the fiber vector onto the transverse plane. The angle between the transverse plane and the projection of the laminar normal vector onto the radial-longitudinal plane is B'_N . The angle between the longitudinal-radial plane and the projection of the laminar normal vector onto the transverse plane B''_N .

III. RESULTS

A. Accuracy of DT-MRI and Sensitivity of ST/HR-MRI and of DT-MRI to Time Post-Fixation

This was initially explored with 6-direction DT-MRI and $b = 1000$ and the analysis is shown in Fig. 1 and Fig. 2. DT-MRI fiber orientation measurement is shown to be highly accurate by comparison to ST/HR-MRI with a difference of 5° or less across $>70\%$ of the wall, and an average difference of 5.4 ± 13.5 for $\Delta\alpha^H$ and 4.1 ± 15.2 for $\Delta\alpha^T$ for the first DT-MRI scan (annotated as scan 1 in Table I, see Table II for results from other scans). DT-MRI laminar orientation measurement, however, has low accuracy compared to ST/HR-MRI, with the minimum difference of 7° and a difference of 20° or greater across 50% of the wall (see Fig. 1 & Fig. 2) and an average difference of $24.2 \pm 31.3^\circ$ for $\Delta\beta'_N$ and $22.2 \pm 27.2^\circ$ for $\Delta\beta''_N$ for the first DT-MRI scan (scan 1 in Table I, see Table II for results from other scans). The standard deviations are large because within the sampled region the sheet angle varies in a complex fashion and can a wide range of values. HR-MRI ST has low sensitivity to time post fixation for all fiber and laminar orientation measures, with a maximum mean deviation $2.9 \pm 11.7^\circ$ between $\Delta\alpha^T$ values (see Table II for average differences in the other orientation measures). Likewise, sensitivity of DT-MRI to time post-fixation is low with similar orientation measures for scans 1, 7 and 11 (other imaging parameters were unchanged between these scans). It can be seen in the following paragraphs and in Table II that these findings also apply qualitatively to 12-direction DT-MRI and across the range of *b*-values explored (500-2500 s/mm^2).

TABLE I. IMAGING PROTOCOL

Scan	Imaging Parameters					
	Start Time ^a	End Time	Type	Directions	<i>b</i> -value (s/mm^2)	Scan Duration ^b
1	2:00	3:50	DT	6	1000	1.83
2	3:50	7:46	DT	12	1000	3.93
3	7:46	9:36	DT	6	1000	1.83
4	9:36	13:32	DT	12	500	3.93
5	13:32	15:22	DT	6	1000	1.83
6	15:22	19:18	DT	12	2000	3.93
7	19:18	21:08	DT	6	1000	1.83
8	21:08	39:20	FL	NA	NA	18.20
9	39:20	41:10	DT	6	1000	1.83
10	41:10	45:06	DT	12	1500	3.93
11	45:06	46:57	DT	6	1000	1.83
12	46:57	65:09	FL	NA	NA	18.20:12
13	65:09	66:59	DT	6	1000	1.83
14	66:59	70:55	DT	12	2500	3.93
15	70:55	72:45	DT	6	1000	1.83

a. time post-fixation, (h:m), a. units (h:m), b. units (hr); DT = DT-MRI, FL = FLASH.

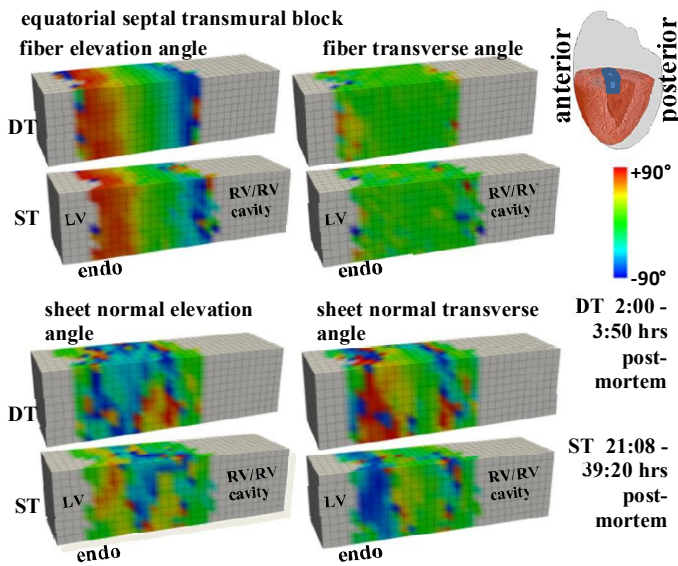


Fig. 1. Myocardial structural orientations in the mid-equatorial septal block, imaged in scan 1 (see Table I). DT - DT-MRI, ST - Structure Tensor analysis of HR-MRI.

B. Sensitivity of DT-MRI to Number of Directions

This was initially explored with $b = 1000$ and the analysis is shown in Fig. 3 and Table II. Sensitivity of DT-MRI to the number of directions is low for both fiber and lamina orientation measurements. As the scans with 6 and 12 directions were carried out at different times post-fixation, the differences in orientations measured are due to a summation of the effects associated with different imaging time and different direction number. It can be seen by comparing Fig. 3 to Fig. 2 that sensitivity to the number of directions is less than to the imaging time. The detailed results for the four orientation measures are shown in Table II. As for sensitivity to time, it can be seen in the following paragraph and in Table II that findings related to the number of directions also apply qualitatively across the range of b -values explored (500-2500 s/mm^2).

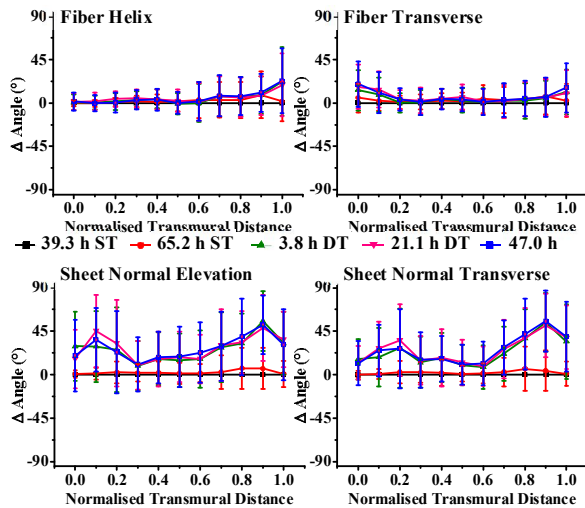


Fig. 2. Transmural angle profiles exploring sensitivity to time (time elapsed from end of perfusion to end of imaging). All orientations are expressed absolute difference to scan number (see Table I).

C. Sensitivity to b -value

This was initially explored with 6-directions and the analysis is shown in Fig. 4. Sensitivity of HR-MRI to b -values in the range 1000 – 2500 s/mm^2 is low with a maximum difference of 14° and an average difference of $\sim 2^\circ$ between all b -values and all orientations measured. However, Fig. 4 shows that DT-MRI with a b -value of 500 s/mm^2 does perform better than DT-MRI with the other b -values explored.

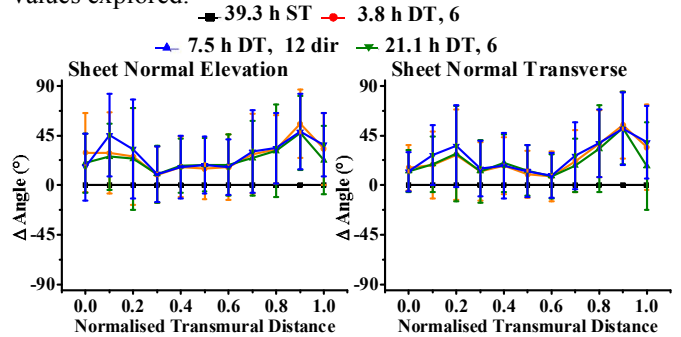


Fig. 3. Transmural angle profiles exploring sensitivity to number of gradient directions (abbreviated as dir here).

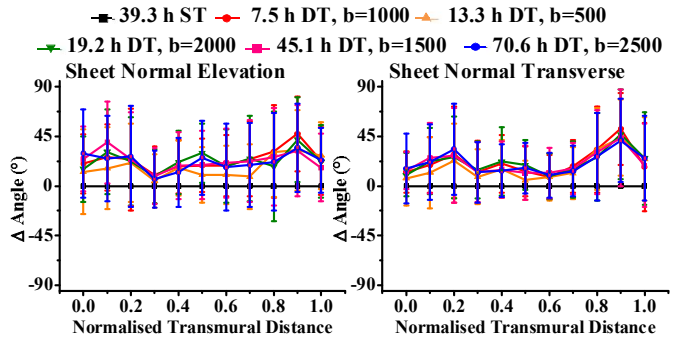


Fig. 4. Transmural angle profiles exploring sensitivity to b -value (in s/mm^2).

TABLE II. SENSITIVITY SUMMARY STATISTICS

T^a	N^b	Parameter	$\Delta\alpha^H(^\circ)$ $m \pm s.d.^d$	$\Delta\alpha^T(^\circ)$ $m \pm s.d.$	$\Delta\beta^H(^\circ)$ $m \pm s.d.$	$\Delta\beta^T(^\circ)$ $m \pm s.d.$
time (parameter = time, h:m, measured from end of fixation)						
S	8	39:20	0	0	0	0
S ^c	1 2	65:09	2.4±11.1	2.9±11.7	2.6±11.7	2.3±11.2
D	1	3:50	5.4±13.5	4.1±15.2	24.2±31.3	22.2±27.2
D	7	21:08	5.7±13.9	5.2±15.7	25.9±30.8	24.6±30.0
D	1 1	46:57	5.9±14.2	5.6±16.4	25.7±32.6	22.4±27.6
number of gradient directions (parameter = number of directions)						
D	1	6	5.4±13.5	4.1±15.2	24.2±31.3	22.2±27.2
D	2	12	6.1±13.3	4.0±14.6	21.9±30.2	18.8±27.7
D	7	6	5.7±13.9	5.2±15.7	25.9±30.8	24.6±30.0
b-value (parameter = b-value, s/mm^2)						
D	4	500	7.2±13.4	4.6±16.7	33.6±60.5	16.7±27.1
D	2	1000	6.1±13.3	4.0±14.6	21.9±30.2	18.8±27.7
D	1 0	1500	7.0±13.3	5.0±15.3	21.3±33.7	18.8±29.1
D	6	2000	7.0±13.3	5.1±15.3	21.5±33.2	19.9±29.0
D	1 4	2500	8.3±14.3	7.1±16.7	20.6±35.8	19.2±29.7

a - T indicates scan type S for ST/HR-MRI, D for DT-MRI; b - scan number, as in Table I; c - all orientations are expressed as absolute difference to scan number 8 (see Table I); d - $m \pm s.d.$ - mean \pm standard deviation

IV. DISCUSSION

We found that there is low sensitivity of either ST or DT myocardial orientation measurements to time post-fixation. This would seem to contradict the findings of [15] who reported progressive changes following transferring fixed tissue to an embedding medium, and hypothesized that this was due to osmotic gradients. We did not transfer the heart from fixation medium to an embedding medium and therefore such osmotic gradients would be minimized. We found that DT-MRI fiber orientation measurement is highly accurate compared to ST/HR-MRI (in agreement with our previous studies [16, 18]), and that this measure was not sensitive to time post-fixation, number of directions, or b -value. It has been shown that fiber orientation determined from the fast and slow compartments of intra-voxel diffusion are globally similar, possibly due to micro-vascular orientation coinciding with myofiber orientation [14]. Myofiber orientation measurement by DT-MRI is therefore not affected to a large degree by the monoexponential diffusion simplification underlying DT-MRI. We found that DT-MRI laminar orientation measures differed significantly from ST/HR-MRI, confirming our previous studies [16, 18]) and that this measure was not sensitive to time post-fixation or the number of gradient directions. Interestingly, DT-MRI performed moderately better at low b -values ($b=500$ s/mm²) than at higher b -values ($b=1000-2500$, s/mm²). It was predicted by [12] that laminar measurement would be more accurate at high b -values and the reason that our results show the opposite is not known. How our findings will influence myocardial measurement will depend on the accuracy required. High accuracy may be required for modeling of myocardial mechanics, and may be less important for modeling electrophysiology where electrophysiological simulations may be insensitive to precise structural organization in some circumstances [19]. A limitation of this study is that currently one region of one rat heart has been quantified. Future studies will extend this to more cardiac locations and more hearts. The current study only investigates DT-MRI on 200 μ m isotropic voxels with 6 or 12 gradient directions. Other diffusion imaging models (e.g. High Angular Resolution Diffusion Imaging) may perform better. Other studies have found sensitivity to imaging parameters (e.g. [20] to b -value in brain). The organ imaged, and the physiological/post-mortem state of the tissue is likely to be an important determinant of sensitivity. To our knowledge this is the first sensitivity analysis of cardiac DT-MRI with direct comparison to macroscopic tissue structural measurements.

REFERENCES

- [1] K. D. Costa, Y. Takayama, A. D. McCulloch, and J. W. Covell, "Laminar fiber architecture and three-dimensional systolic mechanics in canine ventricular myocardium," *Am J Physiol*, vol. 276, pp. H595-607, Feb 1999.
- [2] S. H. Gilbert, A. P. Benson, P. Li, and A. V. Holden, "Regional localisation of left ventricular sheet structure: integration with current models of cardiac fibre, sheet and band structure," *Eur J Cardiothorac Surg*, vol. 32, pp. 231-49, Aug 2007.
- [3] R. Stones, S. H. Gilbert, D. Benoist, and E. White, "Inhomogeneity in the response to mechanical stimulation: cardiac muscle function and gene expression," *Prog Biophys Mol Biol*, vol. 97, pp. 268-81, Jun-Jul 2008.
- [4] D. A. Hooks, M. L. Trew, B. J. Caldwell, G. B. Sands, I. J. LeGrice, and B. H. Smaill, "Laminar arrangement of ventricular myocytes influences electrical behavior of the heart," *Circ Res*, vol. 101, pp. e103-12, Nov 9 2007.
- [5] A. J. Pope, G. B. Sands, B. H. Smaill, and I. J. LeGrice, "Three-dimensional transmural organization of perimysial collagen in the heart," *Am J Physiol Heart Circ Physiol*, vol. 295, pp. H1243-H1252. Epub 2008 Jul 18., 2008.
- [6] N. A. Trayanova, "Whole-heart modeling: applications to cardiac electrophysiology and electromechanics," *Circ Res*, vol. 108, pp. 113-28, Jan 7 2011.
- [7] P. Helm, M. F. Beg, M. I. Miller, and R. L. Winslow, "Measuring and mapping cardiac fiber and laminar architecture using diffusion tensor MR imaging," *Ann N Y Acad Sci*, vol. 1047, pp. 296-307., Jun 2005.
- [8] D. F. Scollan, A. Holmes, J. Zhang, and R. L. Winslow, "Reconstruction of cardiac ventricular geometry and fiber orientation using magnetic resonance imaging," *Ann Biomed Eng*, vol. 28, pp. 934-44., Aug 2000.
- [9] E. W. Hsu, A. L. Muzikant, S. A. Matulevicius, R. C. Penland, and C. S. Henriquez, "Magnetic resonance myocardial fiber-orientation mapping with direct histological correlation," *Am J Physiol*, vol. 274, pp. H1627-34., May 1998.
- [10] G. L. Kung, T. C. Nguyen, A. Itoh, S. Skare, N. B. Ingels, Jr., D. C. Miller, *et al.*, "The presence of two local myocardial sheet populations confirmed by diffusion tensor MRI and histological validation," *J Magn Reson Imaging*, vol. 34, pp. 1080-91, Nov 2011.
- [11] S. H. Gilbert, D. Benoist, A. P. Benson, E. White, S. F. Tanner, A. V. Holden, *et al.*, "Visualization and quantification of whole rat heart laminar structure using high-spatial resolution contrast-enhanced MRI," *Am J Physiol Heart Circ Physiol*, vol. 302, pp. H287-98, Jan 1 2012.
- [12] E. W. Hsu, D. L. Buckley, J. D. Bui, S. J. Blackband, and J. R. Forder, "Two-component diffusion tensor MRI of isolated perfused hearts," *Magn Reson Med*, vol. 45, pp. 1039-45., 2001.
- [13] J. R. Forder, J. D. Bui, D. L. Buckley, and S. J. Blackband, "MR imaging measurement of compartmental water diffusion in perfused heart slices," *Am J Physiol Heart Circ Physiol*, vol. 281, pp. H1280-5., 2001.
- [14] J. B. Bassingthwaite, T. Yipintsoi, and R. B. Harvey, "Microvasculature of the dog left ventricular myocardium," *Microvasc Res*, vol. 7, pp. 229-49, Mar 1974.
- [15] P. W. Hales, R. A. Burton, C. Bollensdorff, F. Mason, M. Bishop, D. Gavaghan, *et al.*, "Progressive changes in T(1), T(2) and left-ventricular histo-architecture in the fixed and embedded rat heart," *NMR Biomed*, vol. 24, pp. 836-43, Aug 2011.
- [16] S. H. Gilbert, G. B. Sands, I. J. LeGrice, B. H. Smaill, O. Bernus, and M. L. Trew, "A framework for myoarchitecture analysis of high resolution cardiac MRI and comparison with diffusion Tensor MRI," *Conf Proc IEEE Eng Med Biol Soc*, vol. 2012, pp. 4063 - 4066, 2012.
- [17] A. P. Benson, S. H. Gilbert, P. Li, S. M. Newton, and A. V. Holden, "Reconstruction and Quantification of Diffusion Tensor Imaging-Derived Cardiac Fibre and Sheet Structure in Ventricular Regions used in Studies of Excitation Propagation," *Mathematical Modelling of Natural Phenomena*, vol. 3, pp. 101-130, 2008.
- [18] S. H. Gilbert, M. L. Trew, B. H. Smaill, A. Radjenovic, and O. Bernus, "Measurement of Myocardial Structure: 3D Structure Tensor Analysis of High Resolution MRI Quantitatively Compared to DT-MRI," *Statistical Atlases and Computational Models of the Heart*, 2012.
- [19] F. Vadakkumpadan, H. Arevalo, C. Ceritoglu, M. Miller, and N. Trayanova, "Image-based estimation of ventricular fiber orientations for personalized modeling of cardiac electrophysiology," *IEEE Trans Med Imaging*, vol. 31, pp. 1051-60, May 2012.
- [20] M.-C. Chou, E.-F. K. Kao, and M. Susumu, "Effects of b -Value and Echo Time on Magnetic Resonance Diffusion Tensor Imaging-Derived Parameters at 1.5 T: A Voxel-Wise Study," *Journal of Medical and Biological Engineering*, vol. 33, pp. 45-50, 2013.